Ultrafast nonexponential dynamics in a polymer glass forming liquid

Abhijit Sengupta and M. D. Fayer
Department of Chemistry, Stanford University, Stanford, California 94305

(Received 29 July 1993; accepted 28 September 1993)

The orientational dynamics of phenyl side groups in poly(methylphenylsiloxane) (PMPS) melts are examined over a broad range of viscosity/temperature (η/T) using subpicosecond transient grating optical Kerr effect (TGOKE) measurements. Measurements on poly(dimethylsiloxane) are also reported. Following ultrafast (hundreds) of fs librational dynamics, the phenyl side group orientational dynamics occur over a range of times from 2 ps to a few hundred ps. The experiments were performed from 25 to 143 °C, resulting in η/T changing by a factor of 40. In spite of the large change in η/T, the side group dynamics remain unchanged throughout the entire temperature range. Comparison of the dynamics of PMPS in the melt and PMPS in dilute CCl_4 solution shows that chain–chain interactions influence the phenyl side group dynamics in the melt. The dynamics are described as local orientational relaxation of phenyl groups in the microenvironments defined by the backbone geometry and side group steric interactions rather than rotational diffusion. The dynamics exhibit power-law behavior, $t^{-\alpha}$, over two decades of signal decay. Two possible physical processes that can give rise to a power-law decay are discussed. The relationship of the observed dynamics to the β and α relaxations of glass forming liquids is also discussed.

I. INTRODUCTION

In this paper, we report the observation of ultrafast orientational dynamics of the phenyl side groups in the polymer melt of poly(methylphenylsiloxane) (PMPS). PMPS is a very flexible polymer with a polar siloxane backbone. Its glass transition temperature, T_g=228 K. The experiments were conducted over a broad temperature range, 25 to 143 °C, using the transient grating optical Kerr effect (TGOKE) method. Over this broad temperature range, the ratio of the viscosity to the temperature η/T changes by a factor of 40. However, the orientational dynamics of the phenyl side groups are independent of temperature throughout the entire temperature range. Experimental results on poly(dimethylsiloxane) (PDMS) are also reported. Comparison of the PMPS and PDMS data demonstrate that the observed temperature-independent orientational dynamics of PMPS arise from motions of the phenyl side groups. Observation of η/T independent dynamics in a liquid are at odds with the simple hydrodynamic model of rotational diffusion which states that the decay time of the orientational correlation function via rotational diffusion is proportional to η/T [the Debye–Stokes–Einstein (DES) equation].[1]

In liquids, local structural relaxation occurs over a broad range of time scales. It is well established that the liquid to glass transition is dynamic in origin.[2,3] With respect to the time window of most spectroscopic techniques, structural disorder in a glass forming liquid freezes in at the glass transition temperature.[4] Especially in a fragile glass forming liquid,[5] a bimodal distribution in the relaxation spectrum exists over a wide temperature range above T_g.[2-4] On approaching T_g from higher temperature, the relaxation process bifurcates into slow and fast relaxation branches below a temperature T_c. This is referred to as a dynamical phase transition. The low-frequency structural relaxation is known as α relaxation.[4] The α relaxation diverges, becoming infinitely slow, near T_g. This divergence is responsible for freezing the spatial inhomogeneity in a glass. Besides the quasiharmonic phonon-like modes, there exists a high-frequency relaxation branch known as β relaxation.[4] α relaxation is a slow, highly temperature-dependent, and q-dependent (wave vector dependent) structural relaxation,[2,3] while β relaxation is a fast, only weakly temperature-dependent, and q-independent local fluctuation.[4] These features of β relaxation are in accord with the mode coupling theories and are experimentally observed in some fast time scale measurements, e.g., neutron scattering and depolarized light scattering experiments (see Sec. III). At low frequency, e.g., dielectric relaxation measurements, the β process also appears as a broad distribution of relaxation rates. The low-frequency β process depends on temperature. However, the temperature dependence is very mild relative to that of the α relaxation observed in the same experiment.[5] In a polymer glass, structural disorder originates from innumerable combinations of backbone conformations and side group orientations. Due to connectivity of the bonds, restricted bond angles, and steric interactions of the side groups, backbone orientational diffusion is orders of magnitude slower than pure side group motions. Backbone motions are responsible for α relaxation in polymers melts.[6,7] They are very sensitive to temperature change and often yield dynamical observables that display stretched exponential time dependence.[6,7] Some experiments[8] suggest that localized motions of polymer side groups are responsible for high-frequency β relaxation and act as precursors to α relaxation.

Dynamics of a fluid system can be described in terms of the density correlation function and the current correlation function.[9] Various types of intramolecular and intermolecular motions participate in the density fluctuation of

 0021-9606/94/100(2)/1673/11/$6.00

a liquid. There are a variety of spectroscopic techniques that probe the scattering function or the density correlation function. Neutron scattering (NS) measures the Fourier transform of the density correlation function $\langle \rho_{-q}(0)\rho_q(t)\rangle$ in the frequency domain. The TGOKE technique, dynamic light scattering (DLS), and Raman spectroscopy examine the correlation of molecular polarizability associated with a dynamic mode or modes responsible for the density fluctuation. Low-frequency Raman spectroscopy probes single molecule reorientation in liquids,[10,11] while the DLS and the TGOKE techniques can give additional information about collective and cooperative molecular reorientation. Within the framework of linear response theory,[10] DLS and TGOKE experiments contain the same information.[12] In TGOKE experiments, the signal comes from Bragg diffraction of the probe beam by a single Fourier component (amplified by the excitation pulses) of the spontaneous dielectric fluctuation of the medium. Decay of the signal corresponds to the quasielastic central peak in DLS and gives information about molecular reorientation. While in principle, DLS and the TGOKE experiment provide the same information, in practice, the grating experiment has tremendous advantages for the measurement of fast and ultrafast phenomena. TGOKE measurements have been made over 6 decades of time and 12 decades of signal intensity.[13] As with many time domain analogs of frequency domain experiments, there are large advantages in the signal-to-noise (S/N) ratio. In DLS it is difficult to resolve very fast components of multitime scale dynamics because the fastest components can appear as an essentially flat base line. DLS measures the projections of polarizability correlation function like $\langle \alpha_{ij}(t)\alpha_{ij}(0)\rangle (i=j$ for VV configuration and $i\neq j$ for VH configuration). In TGOKE experiments, polarization selectivity allows one to measure additional projections of the third-order nonlinear susceptibility $\chi^{(3)}$ such as χ_{1122} or χ_{1222} which are proportional to $\langle \alpha_{11}(t)\alpha_{22}(0)\rangle$ or $\langle \alpha_{12}(t)\alpha_{22}(0)\rangle$, respectively.[12] In the experimental section, the manner in which polarization selectivity of TGOKE method provides information about molecular dynamics in liquids on subpicosecond and picosecond time scales is discussed.

In a recent publication, we reported a study of the femtosecond and picosecond orientational dynamics of the naphthyl side groups of poly(2-vinylnaphthalene) (P2VN)[14] in CCl_4 solution using the femtosecond TGOKE technique. P2VN has a nonpolar backbone and is not very flexible because of steric interactions among adjacent bulky napththyl groups. This lack of flexibility is demonstrated by the high glass transition temperature $T_g = 424$ K. Naphthyl group orientational relaxation in P2VN/CCl_4 solution shows no η/T dependence and, therefore, does not obey the DSE equation.[1] The results of the P2VN study have some features in common with the results presented below. To explain these results, we invoked the concept of local structure relaxation on a fixed local potential surface. This potential surface is defined by the backbone geometry and the side group steric interactions. The surface appears fixed on a time scale short compared to the time scale for backbone motions. Optical or thermal induced angular displacement of a side group (or side groups) moves the local structure away from the minimum of the local potential surface. Then, the observed orientational dynamics are relaxation on the surface back to the original local structure, not rotational diffusion.

In the following, first the data are discussed qualitatively and a comparison is made between the PMPS and PDMS results. The comparison establishes that the dynamics observed in PMPS arise from phenyl side group motions. The PMPS data are then analyzed using a fitting function that permits the η/T dependence to be illustrated. The functional form of the time dependence of the data is then considered in more detail. It is shown that the dynamics exhibit a power-law decay over a wide range of time. Comparison to the TGOKE results on PMPS in solution show that interchain interactions in the melt influence the phenyl side group dynamics. Finally, the possible relationship between these results and β and α relaxation in glass forming liquids is briefly discussed.

II. EXPERIMENTAL PROCEDURES

Detailed descriptions of the subpicosecond dye laser system[15] and the TGOKE experimental setup[16] employed in these experiments are available elsewhere. The DCM dye laser was tuned to 665 nm to avoid two-photon absorption by the phenyl groups. The laser provided 300 fs, 10 μJ pulses at a repetition rate of 1.75 kHz.

By choosing the proper polarizations of all four beams (three input and the signal beams), it is possible to measure various projections of the third-order nonlinear susceptibility $\chi^{(3)}$ in a TGOKE experiment.[17,18] This permits the selective probing of different dynamic processes contributing to the formation and relaxation of a grating. Following the notation of Deeg *et al.*,[18] we define the configuration of the grating experiment as $(0°/\alpha/90°/\beta)$ where the four quantities within the parentheses stand for the angle of polarization of the two excitation beams, the probe beam and the detected signal beam, respectively. All the angles are in reference to the polarization of the excitation beam nearest the probe beam. Molecular orientation optical Kerr effect (OKE) data (referred to as the nuclear OKE) were taken using the (0°/45°/90°/135°) configuration, which detects, $\chi_n^{(3)}$. The (0°/45°/90°/56°) configuration detects the electronic OKE signal. This is the instantaneous polarization of the electrons, and does not contain a contribution from the nuclear OKE. The electronic OKE is used as an instrument response. It is a three pulse correlation and provides an accurate method for determining the pulse duration and shape.[15] Before and after each nuclear OKE measurement of short time dynamics ($t<3$ ps), an electronic scan was taken.[16,18] This assured that the pulse shape was known when the data were analyzed. At longer time ($t>3$ ps), the polarization grating configuration (0°/90°/90°/0°) was employed to obtain the best S/N ratios.[19] The advantages of different grating configurations are discussed in a previous paper.[18] The grating period was 2.5 μm. Spot sizes of the excitation and probe beams were 120 and 70 μm respectively. Typical excitation and probe pulse energies were 100 nJ to 2 μJ and 50 nJ to 0.5 μJ,

respectively. Extensive studies of laser intensity dependence were performed to assure that there were no artifacts. The signal varied linearly in the intensity of each beam with an overall I^3 dependence on the laser intensity. The beams were not depolarized passing through the sample individually.

One of the excitation beams or the probe beam was chopped and the signal was detected by a thermoelectrically cooled PMT. On each laser shot, the output of the PMT was measured by a gated integrator. A computer controlled the scanning of a stepper motor delay line, performed analog-to-digital conversions of a gated integrator output, and averaged the data over several scans. The intensity of each laser shot was also measured, and data from shots outside of a 10% window were rejected. The scattered light level is measured by blocking (chopping) a beam farthest from the signal every other shot. This beam does not contribute to the scattered light. The measured scattered light is normalized by the ratio of the laser intensity on the signal shot and the scattered light shot, and the normalized scattered light is subtracted from the amplitude measured on the signal shot.

Poly(methylphenylsiloxane) (Aldrich), poly(dimethylsiloxane) (Aldrich), and CCl_4 (Baker, for UV spectrophotometry) were used without further purification. PMPS supplied by Aldrich were not synthesized with a particular tacticity. The molecular weight of PMPS is 2600. The concentration of the PMPS/CCl_4 solution was 0.8 M with respect to phenyl groups at 25 °C. The solution was filtered through Gelman 0.2 μm Acrodisk CR filters to remove dust particles. The solution sample was sealed in a 1 mm spectrophotometric cell to prevent evaporation of the solvent. It was not necessary to seal the melts. For measurements above room temperature, the sample cell was mounted inside an aluminum block heated by resistive heating wire. The temperature was regulated using a temperature controller and held constant to ±0.1 °C. The kinematic viscosity was measured using a Cannon–Ubbelohde semimicrotype viscometer as a function of temperature. To obtain the zero frequency shear viscosity at any particular temperature, the measured kinematic viscosity is multiplied by the density of the PMPS liquid. The temperature dependence of the density was also measured.

III. RESULTS AND DISCUSSION

Dynamics observed with TGOKE experiments start with an anisotropy induced in the sample by the excitation beams. The coupling of the radiation field to the molecules involves stimulated Raman scattering exciting librational motions[20–24] of the phenyl side groups. Librations are localized angular vibrations. (The librational motions of the side groups almost certainly have associated with them a translational displacement. However with this in mind, we will use the term libration, the conventional terminology.) These essentially harmonic motions are modes of the potential surface associated with the fixed local structure of the polymer that exists on the ultrashort time scale of the excitation pulses. Because the pulses are short, they have a broad frequency band width ($\sim$100 cm^{-1}). Thus, the pulses contain both frequencies necessary to excite the low-frequency (a few tens of cm^{-1}) librations by stimulated Raman scattering. The orientation of the excited librations is determined by the polarization of the excitation radiation field. Therefore, the laser excited librations add to the isotropic distribution of thermally excited librations, making the ensemble of excited librations anisotropic. The initial ultrafast transient (a few 100 fs) seen in TGOKE experiments consists of a rise in the signal as the overdamped librators begin to undergo angular displacement and the partial (or complete) decay of the signal as the librational motion dephases and damps. In a dense liquid, correlated motions of pairs, triplets, etc., of molecules can also be driven to some extent and will lead to a very short-lived contribution to the signal through interaction induced polarizabilities.[25,16]

In a crystal, stimulated Raman scattering excites optical phonons. Because of the well-defined lattice structure, damping of the optical phonons returns the molecules to their original positions, leaving no residual anisotropy. In a liquid polymer, damping of the optically excited librations can result in orientational displacements from the initial configurations. This leaves a longer lived residual anisotropy that will decay by some form of orientational relaxation. In a simple liquid, such as biphenyl,[16] one observes the fast librational motions and a biexponential decay of the residual anisotropy. The long-lived anisotropy decays by orientational diffusion, and both components of the biexponential obey the DSE equation.

The Bragg scattered intensity $S(t)$ of a probe pulse delayed by time t with respect to the excitation pulses is given by

$$S(t)=\int_{-\infty}^{+\infty} dt'' I_p(t''-t) \times\left[\int_{-\infty}^{t''} G^{\epsilon\epsilon}(t''-t')I_e(t')dt'\right]^2, \tag{1}$$

where $G^{\epsilon\epsilon}(t)$ is the impulse response function (Green function) of the liquid's dielectric tensor for ultrashort optical pulse excitation, and $I_e(t)$, and $I_p(t)$ are the intensity profiles of the excitation and probe pulses, respectively. The impulse response function $G^{\epsilon\epsilon}(t)$ is related to $C^{\epsilon\epsilon}(t)$, the time correlation function of the collective polarizability of the liquid at a fixed $\mathbf{q}$ (grating wave vector),[12]

$$G^{\epsilon\epsilon}(t)=-\frac{\Theta(t)}{k_BT}\frac{\partial}{\partial t}C^{\epsilon\epsilon}(t). \tag{2}$$

$\Theta(t)$ is a unit step function, and the dielectric time correlation function is

$$C^{\epsilon\epsilon}_{ijkl}(t)=\langle\delta\epsilon_{ij}(0)\delta\epsilon_{kl}(t)\rangle.$$

In Eq. (2), the $1/k_BT$ term normalizes the magnitude of the signal and does not influence the time dependence.[27] Equation (2) can only be applied to an arbitrary analytic function $G^{\epsilon\epsilon}(t)$ if the complex function $G^{\epsilon\epsilon}(\omega)$ [Fourier transform of $G^{\epsilon\epsilon}(t)$] is regular in the upper half plane.[27] The instrument response is convolved analytically with a model response function to fit the fs nuclear OKE

data,[14–16] yielding the decay time constants of the librational modes. Here, we are interested in the longer lived component of the grating induced anisotropy. The ultrashort time scale behavior (<1 ps) will be considered qualitatively. It is not necessary to perform convolutions to analyze the longer time scale data that will be discussed quantitatively.

To improve the signal-to-noise ratio, at $t>3$ ps, the polarization grating configuration is used.[14,18,19] The polarization grating configuration is equivalent to the frequency domain VH measurements in depolarized light scattering experiments. For small molecules in dilute solutions or in low viscosity neat liquids, VH measurements of DLS give rotational diffusion times that obey the DSE equation.[1,28] In the viscosity range where the shear relaxation is much faster than the orientational relaxation, the DSE equation is obeyed. In dense fluids, the VH spectra become complicated due to coupling of reorientation, local translation, and shear relaxation.[9,28–31] At times sufficiently long that convolution is unnecessary ($t>1$ ps), the TGOKE signal is proportional to the square of the sample response function, $G^{\epsilon\epsilon}(t)$:

$$S(t) \propto [G^{\epsilon\epsilon}(t)]^2. \tag{3}$$

Figure 1 compares the TGOKE signal from a PMPS melt (a) and a PDMS melt (b) at short times. The polarizations used give only nuclear OKE data; the electronic contribution to the OKE is suppressed.[18] The PMPS signal is 400 times stronger than the PDMS signal near $t=0$. [The data in the main section of b has been multiplied by 400.] The insets in Figs. 1(a) and 1(b) display data on a longer time scale. The signal magnitudes in the (a) and (b) insets are amplified by a factor of several thousand relative to the main parts of (a) and (b), respectively. While PMPS (a) displays a substantial long-lived signal running out to many tens of ps, PDMS (b) displays no detectable signal after ~ 1 ps. PDMS exhibits zero residual anisotropy following the librational damping. In contrast, the residual anisotropy is very large after the librational damping in PMPS, and its decay is highly nonexponential. The phenyl side groups in PMPS are very polarizable and have a large anisotropy in their polarizability. The observations that the PMPS signal is 400 times stronger than the PDMS signal and PMPS displays residual anisotropy for times longer than 1 ps demonstrate that the PMPS signal comes predominately from the phenyl side groups at short times and exclusively from the phenyl side groups at longer times. When the PDMS librations damp, the system is left essentially in its original configuration. However, following the damping of the PMPS librations, the phenyl side groups have not returned to their original orientations. The phenyl side group residual orientational anisotropy decays on the time scale >1 ps.

Figure 2 displays the PMPS long-lived anisotropy decay at two temperatures, 25 and 90 °C. The data are shown from 3 to 300 ps. In the inset, the data are displayed from 20 to 300 ps, and the data have been amplified. The data sets taken at all temperatures are absolutely superimposable in spite of the fact that the measured zero frequency

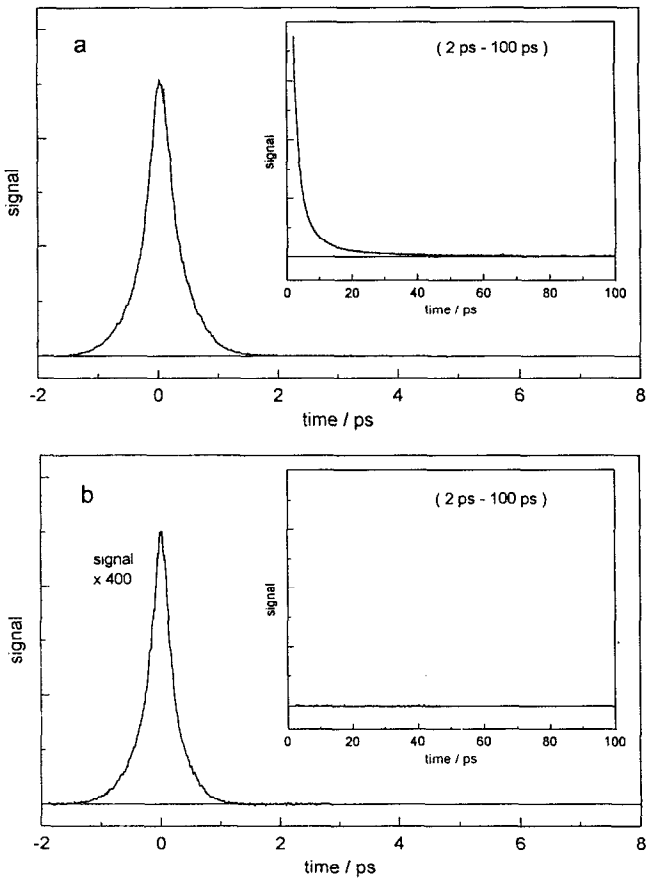

FIG. 1. Transient grating optical Kerr effect (TGOKE) signal of the poly(methylphenylsiloxane) (PMPS) melt is contrasted with that of the poly(dimethylsiloxane) (PDMS) melt. The data reflect molecular orientational dynamics only; the electronic contribution to the OKE is suppressed by polarization-selectivity. (a) Typical TGOKE signal of the PMPS melt. The dynamics at short time (<1 ps) arise from librational excitation and damping (dephasing). The inset (the data are multiplied by 1000 relative to the main figure) shows the decay of a large residual anisotropy left after librational damping. (b) The TGOKE signal of the PDMS melt is 400 times weaker than that of the PMPS melt. [The data are multiplied by 400 relative to the data in (a).] The data in the inset are multiplied by 1000 relative to the main part of (b). There is no detectable signal, i.e., no residual anisotropy, after 1 ps.

shear viscosity changes by a factor of greater than 20 over this range of temperatures, and η/T changes by more than a factor of 40.

To obtain a more quantitative description of the influence of temperature and viscosity on the phenyl group orientational dynamics, the data at a variety of temperatures were decomposed into a sum of exponentials. The data for $t>3$ ps can be fit with the response function $G^{\epsilon\epsilon}(t)$ expressed as a sum of three exponentials,

$$G^{\epsilon\epsilon}(t) = A_f \exp(-t/\tau_f) + A_l \exp(-t/\tau_l) + A_s \exp(-t/\tau_s). \tag{4}$$

Equation (4) is a fitting function used to permit a detailed comparison among data sets taken at different temperatures. A discussion of the functional form of the data is given below. The data sets were fit to the square of Eq. (4)

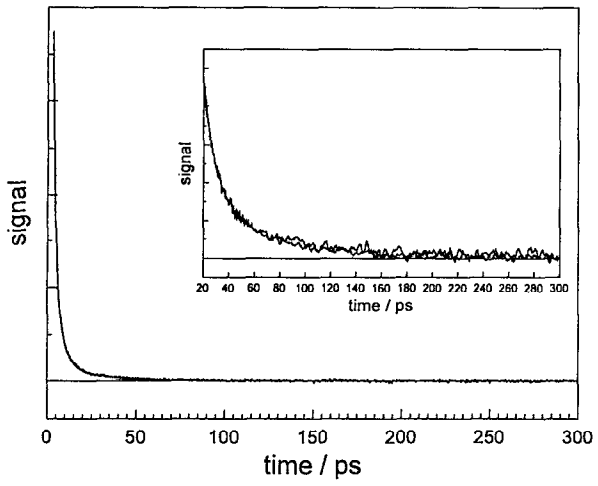

FIG. 2. TGOKE data of the PMPS melt at two different temperatures, 25 and 90 °C, are perfectly superimposable. This shows that the orientational relaxation of the phenyl side groups is viscosity/temperature independent in spite of the large change in viscosity over this temperature range.

[see Eq. (3)]. Also, exponential decomposition of the data sets were employed. To perform the exponential decomposition, the slowest component is fit. The square root of the entire data set is taken, and the square root of the slowest component is subtracted. Since the experiment measures the square of the sample response function [Eq. (3)], the square root is taken to eliminate cross terms in the decomposition. The intermediate decay is subtracted to yield the fast portion. The fast and intermediate decay components can be followed for nine and six factors of e of signal decay. The slowest component does not have as large a dynamic range as the intermediate and fast components and was determined most accurately by the full triexponential fit to the data. The decay times obtained from the triexponential fits are ($f \equiv$fast; $i \equiv$intermediate; $s \equiv$slow) are $\tau_f = 2.3 \pm 0.2$ ps, $\tau_i = 11.5 \pm 1$ ps, and $\tau_s = 105 \pm 10$ ps. Error bars were determined by the spread of fits over many separate data sets.

In Fig. 3, the fast, intermediate, and slow decay components of the triexponential fit are plotted vs η/T. This figure clearly shows the total lack of dependence of the dynamics on η/T on all the observed time scales. The viscosity data, displayed in Fig. 4, obey a Vogel–Fulcher–Tammann (VFT) equation.[4,32] (See Fig. 4 caption.) The parameter T_0 is ($T_g - 20°$), typical of many glass forming liquids. For glass forming liquids, a dynamical phase transition, observed as a bifurcation of relaxation times (see discussion in Sec. I), occurs below a certain temperature T_c which is well above T_g. Measurement of T_c is difficult. For many small molecule organic supercooled liquids, it is found that $T_c/T_g \approx 1.2$–1.3 and $\eta > 10^2$ P in the bifurcation regime below T_c.[33] The temperature range of the PMPS experiments is 1.3–1.82 T_g and the viscosity regime is $10\ \mathrm{P} > \eta > 10^{-1}$ P. Since PMPS is a polymer, it is possible that T_c is much higher than for small molecule liquids. The observed VFT temperature dependence of the viscosity, as shown in Fig. 4, is a characteristic feature of small molecule liquids in the regime where the relaxation processes

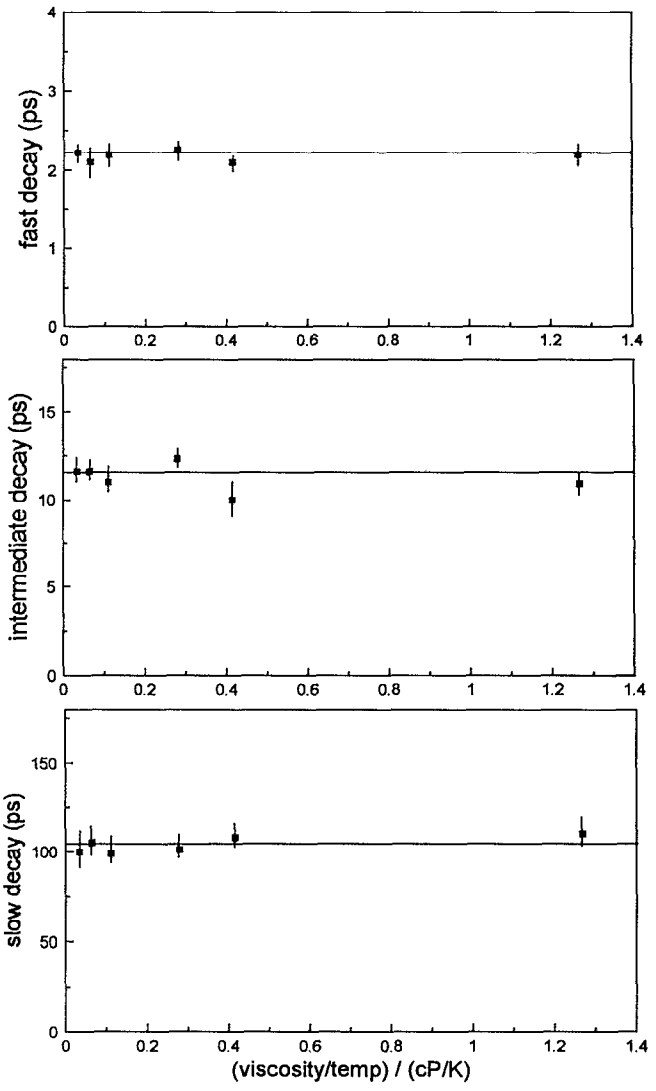

FIG. 3. The fast (τ_f), the intermediate (τ_i), and the slow decay (τ_s) components of phenyl group orientational relaxation in PMPS melts as a function of viscosity/temperature (η/T). The results clearly demonstrate that the dynamics are completely independent of η/T. The Debye–Stokes–Einstein equation for hydrodynamic rotational diffusion predicts a change of a factor of ~40 over the range of η/T displayed.

are bifurcated into α and β relaxations.[33] The lack of temperature dependence of the observed decays suggests that these are related to the β process. Over the temperature range studied, PMPS is viscoelastic[34,35] and the width of the Brillouin peak (the rate of acoustic damping) varies substantially with temperature.[34] The fact that the orientational dynamics of the phenyl side groups are independent of temperature and viscosity over such a broad range of η/T (a factor of 40) demonstrates that the dynamics are decoupled from the low-frequency hydrodynamic modes. The lack of viscosity and temperature dependence of the PMPS phenyl side group dynamics in the pure polymer melt is analogous to the recently reported η/T independent orientational dynamics of the naphthyl side groups of poly(2-vinylnaphthalene) in dilute solution[14] and the η/T independent dynamics of several other systems.[13,19,36,37]

As discussed above, the triexponential function was

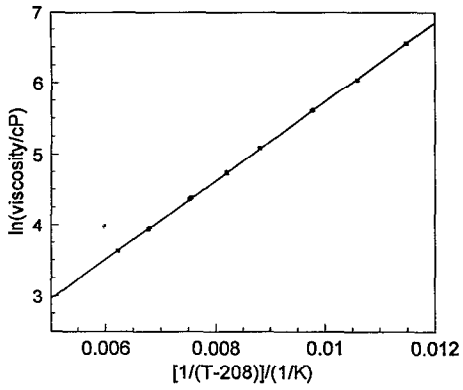

FIG. 4. Over the temperature range of these experiments, the shear viscosity of the PMPS melt obeys a Vogel–Fulcher–Tammann equation: $\eta=\eta_0 \exp[DT_0/(T-T_0]$ with $T_0=208$ K.

used as a fitting function and does not correspond to the true functional form of the TGOKE decay. Figure 5 shows a log–log plot of the data from 3 to 300 ps. A straight line (dashed line) is drawn through a portion of the data. The data appear linear on the log–log plot from ~10 to 300 ps, spanning two decades of signal decay. A straight line on a log–log plot indicates that the functional form of the data is a power law, $t^{-\alpha}$. A faster component is observed for times less than 10 ps. The data at all temperatures examined in these experiments have the identical shape within a very small experimental error (see Figs. 2 and 3). In Fig. 6, the same data are plotted with a fit (dashed curve) to the function

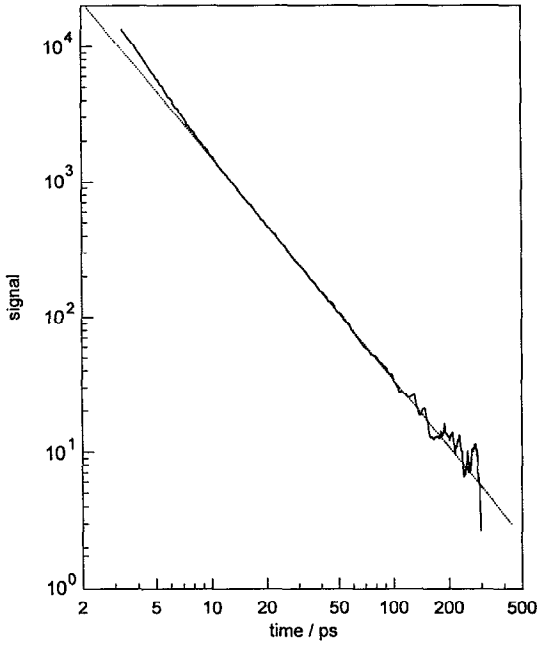

FIG. 5. A log–log plot (base 10) of the data from 3 to 300 ps. A straight line (dotted line) is drawn through a portion of the data. The data appear linear on the log–log plot from ~10 to 300 ps, indicating that the functional form of the data is a power law, $t^{-\alpha}$. A faster component is observed for times less than 10 ps.

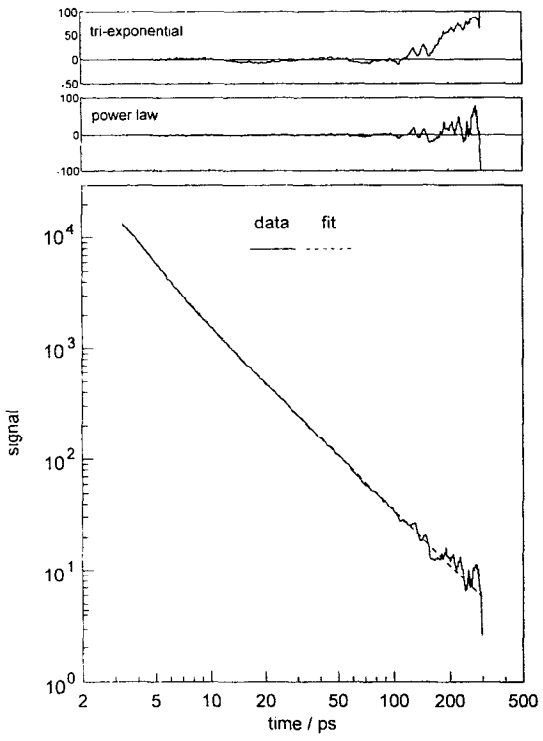

FIG. 6. The same data as in Fig. 6 and a fit with a response function of the form: an exponential plus a power law [Eq. (5)]. The high quality of the data permits a very accurate fit as indicated by the residuals shown at the top (labeled power law). The exponential decay constant $\tau=1.95$ ps and the power-law exponent $\alpha=0.82$. The residuals are calculated as percent deviation of the data from the fit $100\times$(data−fit)/data. The residuals of the fit to the same data with the triexponential response function [Eq. (4)] (labeled triexponential) are also shown for comparison. The triexponential does not reproduce the functional form of the data.

$$S(t) \propto [G^{\epsilon\epsilon}(t)]^2=[A\, e^{-t/\tau}+Bt^{-\alpha}]^2, \tag{5}$$

i.e., the sum of an exponential and a power law. As can be seen from the figure and the residuals (labeled power law), the fit over the entire time range is essentially perfect. In the fit, $\tau=1.95$ ps and $\alpha=0.82$. At the long time limit of the data, there is no tailing off. This implies that the power-law behavior extends to longer times than 300 ps. While the triexponential fit to the data is very useful for displaying the lack of η/T dependence of the fast, intermediate, and slow portions of the data, it does not yield nearly as good a fit as Eq. (5). The residuals of the triexponential fit are shown at the top of Fig. 6. It is clear that the triexponential does not reproduce the functional form of the data as well as Eq. (5). Only the high quality of the data makes the distinction possible.

Since Si–O bonds are polar, the backbone reorientation in PMPS is dielectrically active. The dipole components add up in the direction perpendicular to the backbone.[38] Therefore, dielectric measurements will not be able to observe pure side group reorientation; there will be a contribution from backbone reorientation. The polarization grating TGOKE signal depends on the anisotropy of the polarizability. The data (Fig. 1) demonstrate that the response to the optical excitation of phenyl groups is much

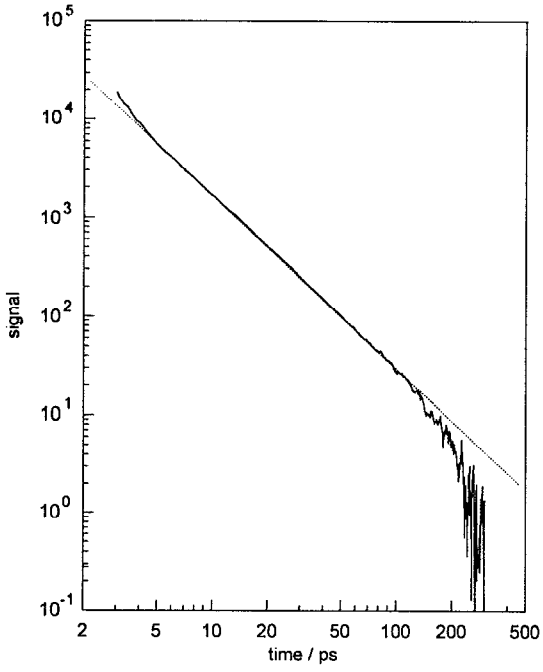

FIG. 7. A log–log plot (base 10) of the dilute solution data (PMPS in CCl_4) with a straight line (dotted line) drawn through it. As in the melt, the data are a power law over a significant portion of the decay. There are differences between the data in the melt and the data in solution which indicate that interchain interactions play a role in the phenyl side group dynamics in the melt.

greater than that of the Si–O–Si backbone or the CH_3 groups. This makes possible the study of pure side group orientational relaxation in PMPS melts. Because of the ultrashort duration of the excitation pulses, negligible anisotropy is induced in the slow dynamic modes involving backbone reorientation (see discussion in Ref. 8). Therefore, the residual anisotropy left after the librational relaxation is due to orientational anisotropy of the phenyl groups. The TGOKE measurements were performed at low q ($q \sim 2.5 \times 10^{-4}$ Å^{-1}). Like DLS experiments, these TGOKE measurements may include contributions from collective reorientation of the phenyl groups.[9,28] For small molecule liquids, experiments on a dilute solutions yield the single molecule reorientation dynamics of the solute molecules. For a polymer in a random dilute solution, side group orientational relaxation will not be influenced by intermolecular interactions with side groups situated on different chains. Collective reorientation of nearby side groups may still contribute to the TGOKE signal in dilute solution.

To determine if the observed phenyl side group dynamics in the melts involve interchain interactions, TGOKE experiments were performed on a dilute solution of PMPS in CCl_4 at 25 °C. Following the librational decay, the orientational dynamics are very similar to the melt, but not identical. Figure 7 shows a log–log plot of the dilute solution data with a straight line (dashed line) drawn through it. As in the melt, the decay is a power law over a significant portion of the decay. However, there are differences between the data in the melt and the data in solution. The exponent in the power law, $\alpha = 0.87$ in solution while it is 0.82 in the melt. These are very close, but given the high quality of the data, they are not identical. A more obvious feature of the solution data is the tailing off at long time. By 100 ps, the data from PMPS in solution are clearly decaying faster than the power law and have the appearance of going over to a slowest exponential component at long time. This is in contrast to the melt data. Finally, the data in solution does not display the same fast exponential component at very short time. In the melt, there is a fast exponential decay ($\tau = 1.95$ ps) that does not merge into the power law until ~ 10 ps. In the solution data, there is also a fast component ($\tau = \sim 0.7$ ps) that merges into the power law by ~ 5 ps.[39] While the differences between the melt data and the solution data are not dramatic, they indicate that interchain interactions play a role in the dynamics of the phenyl side groups in the melt. The extension of the power law to longer times in the melt demonstrates that the continuous range of time scales of dynamic processes extends to longer times. This is probably due to a more complex set of local structures in the melt involving the interaction of the phenyl side groups on one chain with the side groups and backbone of other chains. The differences in the nature of local structures in the melt vs the solution can also be responsible for the observed difference in the α's.

There are many types of mechanisms that can give rise to a power law. Very general, detailed quantum-mechanical descriptions have been given for the relaxation of a perturbation of a noncrystalline material that has some degree of local structure. See, e.g., Dissado *et al.*,[40] and references therein. Concepts presented in the quantum-mechanical treatments apply here as well. Since the energies of the librational oscillators are small compared to kT, the dynamics will be discussed classically. Furthermore, the experiments only observe the anisotropy induced by the excitation fields. Therefore, the isotropic background of thermal excitations need not be considered. We will briefly discuss two well-known models that can give rise to power-law decays. The models are a parallel process and a serial process (hierarchically constrained dynamics model). These models are considered because the physical nature of the PMPS melts suggests that they may be relevant.

The lack of η/T dependence can be attributed to the well-defined local structures that exist for a time much longer than the time scale of the observed relaxations. Similar behavior has been observed in several distinctly different systems.[13,14,19,36] In a crystal, vibrations occur superimposed on a minimum energy background lattice fixed at all times. However, in liquids, the background structure itself is subject to change during librational excitations due to the presence of other configurational states that are close in energy. Recent theoretical calculations of normal modes of liquids[23] revive a concept first put forward by Maxwell,[41] i.e., for times shorter than a characteristic "Maxwell time" τ_m, a liquid behaves in many respects like a solid. Using a method analogous to the harmonic normal mode analysis of solid-state physics, configuration averaged densities of states $\langle \rho(\omega) \rangle$ of liquids have been calcu-

lated.[23] The calculated modes consist of both real and imaginary values of the frequency. The imaginary ω's imply that the structure is unstable on some time scale. The real ω's represent a spectrum of oscillatory modes that are analogous to the phonons of a fixed crystalline lattice. τ_m, the time scale on which the local structure is preserved, is determined by the density of unstable modes. When the density of unstable modes (imaginary ω's) becomes large at $|\omega| \leqslant |\omega_u|$, a significant structural rearrangement would occur at $t \geqslant |\omega_u^{-1}| = \tau_m$.[23] At $t > \tau_m$, the local structure evolves, and the relaxations slower than τ_m should be sensitive to a change of temperature and viscosity.

Through stimulated Raman scattering, the excitation pulses excite a subset of the real frequency spectrum of the PMPS liquid. The potential surface for a particular oscillation of a phenyl side group or groups is determined by local backbone structures and side group steric interactions. The oscillation occurs along a normal coordinate q_l associated with the one-dimensional potential surface for a "normal mode" of the local structure. The l indicates that the potential surface is determined by the local structure that exists on a time scale long compared to the inverse frequency of the oscillation and the time for the relaxation observed in the TGOKE measurements. On a longer time scale, the local structure will evolve. When the oscillator damps, it is left with $q_l \neq 0$. Then the relaxation of this displacement returns the local structure to its initial configuration. This causes the decay of the residual anisotropy observed by the TGOKE experiments following the librational damping. Only on a much longer time scale, the time scale for backbone structure to evolve, will the local structure change significantly. Because of the large number of backbone conformations and chain–chain interactions, there will be a wide variety of phenyl group microenvironments. These will have different potential surfaces, and each microenvironment may have a variety of normal modes existing on the short time scale of the experiment.

A. The parallel process model

The microscopic local structure is altered by the optical field. The relaxation dynamics are associated with the time evolution of the q_l and are determined by the slopes of the microenvironment normal modes' potential energy surfaces, $V(q_l)$'s. For a single normal mode,

$$\frac{dq_l}{dt} = -\kappa \frac{dV(q_l)}{dq_l}, \tag{6}$$

κ is a proportionality constant. For a parabolic surface, the time evolution of q_l is exponential with a decay constant, Γ_l. A distribution of curvatures of the parabolic surfaces for the normal modes in the various microenvironments gives rise to a distribution of Γ_l's. Then the observed decay of the TGOKE signal will be a broad distribution of exponentials. The weight of a particular Γ_l occurring in the distribution is $w(\Gamma_l)$. Integrating over the distribution of decay constants, the observed power-law decay will occur if

$$w(\Gamma_l) = \Gamma_l^{\alpha-1}, \tag{7}$$

i.e.,

$$G^{\epsilon\epsilon}(t) = \int_0^\infty (\Gamma_l^{\alpha-1}) e^{\Gamma_l t}\, d\Gamma_l = \beta t^{-\alpha}, \quad t > 0, \tag{8}$$

where β is a constant.[42] For a finite range of Γ_l, $\Gamma_{\min} < \Gamma_l < \Gamma_{\max}$, the decay is a power law over a limited range of time, $\tau_{\min} < t < \tau_{\max}$. The crossover from a power law to a pure exponential occurs for $t > \tau_{\max}$. To reproduce the observed data, the range of Γ's spans ~ 2.5 orders of magnitude. The experiment yields $\alpha = 0.82$. Therefore, the weighting function for the relaxation rates is $w(\Gamma_l) = \Gamma_l^{-0.18}$.

Distributions of rates of the form of Eq. (7) are seen in other condensed matter systems. For example, in low-temperature glasses, relaxation rates of glassy two-level systems have been observed to have a distribution[43,44] $w(\Gamma) = \Gamma^{-1}$. Recent TGOKE experiments on two liquid crystals in the isotropic phase displayed power-law behavior.[13] When the parallel process model is used to analyze the decays for these systems, both gave $w(\Gamma) = \Gamma^{-0.37}$.

B. The serial process model

In the serial process model, the dynamics of relaxation involves sequential release of constraints in a hierarchy of degrees of freedom.[45,46] A glass forming system can become nonergodic during the time scale of a fast measurement even at $T > T_g$. This implies that simultaneous relaxation of all degrees of freedom cannot happen, and the ensemble average of the relaxation of many microenvironments is not an accurate physical description. Fast dynamics within a smaller set of states bring the system into a configuration that permits somewhat slower dynamics within a larger set of configurations which in turn release constraints that permit even slower dynamics within an even larger set of configurations. Here, the largest set of configurations corresponds to a correlation length of the microenvironment ξ_m and the longest time scale is associated with an ergodic time, $\tau_{\max}$.

Hierarchically constrained dynamics[45] has been proposed as a phenomenological model for non-Debye relaxations, especially in glassy systems. This model will give a stretched exponential decay or a power-law decay depending on the distribution of states in the hierarchy of levels and the conditions for release of constraints to allow the subsequent set of motions.[45,47] The constraints can dominate the relaxation dynamics over a wide time range. Palmer *et al.*[45] demonstrated a model of this type for a distinct series of levels of Ising spins. Here we will use the mathematical formulations of this model to obtain the response function for the relaxation dynamics of a perturbed microenvironment. For a series of n levels with N_n Ising spins or binary fluctuations in a given level, a constraint is imposed on the system such that a relaxation process in the succeeding level $(n+1)$ may not occur unless μ_n elements have attained a particular configuration out of their 2^{μ_n} possible ones in the previous level (n). In PMPS, a number of phenyl groups may generate a large number of orientationally disordered collective configurations. Configura-

tions which are cooperatively interconvertible may constitute a level; and each single step of orientational distortion during interconversion may correspond to a binary fluctuation. (This should not be taken too literally since the process may involve more than a binary fluctuation.) Assuming no intralevel correlation, the relationship between the average relaxation times of Ising spin flip in different levels is obtained:

$$\tau_{n+1}=2^{\mu_n}\tau_n. \tag{9}$$

The microenvironment relaxation and the observable $G^{\epsilon\epsilon}(t)$ is determined by the constraint release dynamics, i.e.,

$$G^{\epsilon\epsilon}(t)=\sum_{n=0}^{\infty} w_n \exp\left(\frac{-t}{\tau_n}\right), \tag{10}$$

where $w_n=N_n/N$. w_n is the weight of the decay with decay constant τ_n in the distribution of decays. N_n is the number of states in the nth level; N is the total number of states.

A power-law decay, as observed in the experiments, will only occur for certain conditions on μ_n and w_n. The weighting is geometric, with $N_{n+1}=N_n/\lambda$, where $\lambda>1$. This weighting is allowed in that $N=\Sigma_{n=0}^{\infty}N_n$ is convergent. If the number of elements that must relax in each level is the same for all levels, $\mu_n=\mu_0$, $\tau_{\max}$ is not finite. At $T>T_g$, there must be a slowest decay for the PMPS liquid. Therefore, we require $\tau_{\max}$ to be finite. Assuming an exponential distribution of the number of elements that must be relaxed to release constraints, $\mu_n=\mu_0\exp(-\gamma n)$, gives a large but finite $\tau_{\max}$ for $\gamma\ll 1$. Using these conditions, $G^{\epsilon\epsilon}(t)$ is a power law for $t<\tau_{\max}$,

$$G^{\epsilon\epsilon}(t)=\beta t^{-(\ln\lambda)/\gamma}=\beta\, t^{-\alpha}. \tag{11}$$

Experimentally, $\ln\lambda/\gamma=0.82$ for the PMPS melt. Since $\gamma\ll 1$, $\lambda\cong 1$. This implies that the number of states per level falls off very slowly with increasing n and therefore many levels participate in the process. The levels and the states are associated with the structure of the microenvironment. This model implies that a number of phenyls, on chain and off chain, interact over some correlation length to form a microenvironment. The optical (or thermal) perturbation modifies the local structure and the relaxation occurs through constraint release.

The above discussions show that either a parallel or a serial relaxation model can account for the observed power-law decay. Based on the data there is no way to select between the two models or other possible processes that can give rise to power laws.[40,48–50] However, in the constraint release picture, at least within its incarnation in terms of the Ising spin model, the observed value of $\alpha=0.82$ implies that there are a great many levels with a large number of states per level. Since the backbone structure is fixed on the time scale of the experiments, this suggests that the levels and states involve configurations of the side groups. To have a very large number of levels each containing a large number of states indicates that the correlation length ξ_m is very large, and therefore that fast (100 ps) correlated dynamics are occurring over long distances. In contrast, the parallel process model only requires that there is a broad inhomogeneous distribution of microenvironments. Since the backbone is very flexible because of the large ionic character of the Si–O bonds, it is reasonable to assume that the phenyl side groups will exist in many structural configurations either in the melt or in solution. Experiments on poly(2-vinylnaphthalene) (P2VN) in CCl_4 solution[14] over a wide η/T range displayed no η/T dependence, just like the PMPS. However, the P2VN data, following the ultrafast librational dynamics, are a true biexponential decay. The decay constants are 0.95 and 9.0 ps. Both components have large amplitudes. P2VN is a carbon backbone polymer that does not have the structural flexibility of PMPS. The bonds are strictly covalent and the geometry is tetrahedral. The biexponential observed in P2VN was described as relaxation on the local potential surface determined by the local backbone geometry and napthyl side group steric interactions. If this is correct, then it suggests that the power law observed in PMPS arises from parallel dynamics but that PMPS has a very broad distribution of local structures, in contrast to P2VN.

In the PMPS melts, following the ultrafast librational dynamics, we observe an exponential decay ($\tau=1.95$ ps) at short time that merges (~ 10 ps) into a power-law decay. Equation (5) gives a remarkably good fit to the data as shown in Fig. 6. Samios and Dorfmuller[3] performed Raman line shape measurements of the reorientation of the C_6 axis of the phenyl group in PMPS ($M_w=2600$, viscosity 500 cP.) They fit the observed line shape to a single Lorentzian and obtain a relaxation time of 2.8 ps. While this is similar to the exponential decay component of the TGOKE data, the difference seems to be too great to assume that the two correspond to the same motion. The Raman line shape provides the decay of the single particle orientational correlation function. The TGOKE experiment is sensitive to single particle and collective orientational relaxations involving any motion that affects the polarizability anisotropy of a liquid.

Dielectric relaxation spectroscopy and quasielastic light scattering studies of PMPS[6,51] observed a temperature-dependent collective relaxation (α relaxation) which can be fit to a stretched exponential form ($\tau_{kww}\sim 10^{-9}$ s). Since dielectrically active relaxation in PMPS originates primarily from the dipole moments of Si–O bonds, α relaxation is believed to involve large-scale backbone reorientation. Neutron scattering studies from polybutadiene,[52] di-2-ethylhexylpthalate (DOP),[53] PMPS,[8] and low-frequency (2–100 cm^{-1}) Raman spectroscopy of $GeSBr_2$[3] observed a high-frequency q-independent, temperature-independent β process. In most cases, the accuracy of the measurements of β relaxation is limited by the time window of the spectroscopic techniques. In any specific case, elucidation of the β relaxation in terms of molecular level dynamics (distance scale of a few Å) is very difficult. Neutron scattering measurements on PMPS[8] indicate coupling of α relaxation to phenyl reorientation above 331 K. NS is unable to observe pure side group motion isolated from the contribution of backbone motions occurring in the same wave vector and

time windows. At lower temperatures, the NS experiments[8] observed a q-independent and temperature independent relaxation (β process). The data are fit to a single Lorentzian and yield an exponential correlation decay time of 30 ± 3 ps. The TGOKE results for the phenyl side group dynamics are a power law from 10 ps past 300 ps. This is the system's impulse response function which is related to the decay of the correlation function. Clearly there are dynamics on the 30 ps time scale, but the TGOKE experiments do not yield an exponential decay in this time window.

When the experimental temperature is changed, the PMPS viscosity changes substantially. (See Fig. 4.) As the viscosity decreases, the time scale for change in the local structure decreases. However, so long as this time scale is long compared to the time scale for relaxation of the perturbed local structure, the local potential surface is fixed, and the rate of relaxation is independent of viscosity. The lack of temperature dependence arises for the same reason. If a change in temperature does not change the local potential surface, the relaxation is temperature independent. Although η/T changes substantially over the experimental range, kT changes only $\sim 35\%$. If there is a temperature dependence to the signal weaker than $\sqrt{T}$, it would not be detectable. There is a small change in density. A change in density can arise from an increased level of excitation of anharmonic oscillators and need not involve a change in the form of the potential governing the phenyl group dynamics. However, if there is a very weak temperature dependence of the local structure, any related temperature dependence of the experimentally observed decay might go undetected.

If the observed η/T independent dynamics are identified with the β relaxations of glass forming liquids and are ascribed to relaxations on local potential surfaces fixed on the time scale of the measurements, then what is the connection to the slow α relaxations? We suggest the following picture that is based on concepts found in the results of simulations of glass forming liquids and in mode coupling theory. Mode coupling theory and molecular dynamics methods indicate that β relaxation involves only a small number of atoms (molecules).[54] The description given above involves the motions of single and small numbers of phenyl side groups relaxing on a local potential surface. In a crystal, excitation of an optical phonon is followed by damping that leaves the system precisely in its initial configuration. There is no residual anisotropy. In the liquid, if the local environment were fixed and static, damping would leave no residual anisotropy. However, it is fluctuations of the local environment about the minimum energy structure that leaves the system displaced from the minimum following the librational damping. A classical harmonic oscillator, overdamped in a viscous medium, if displaced from the origin will relax back to the origin as a biexponential.[55] The two decay rates are related to the oscillator frequency and the viscosity. The decay of the residual phenyl group anisotropy is the equivalent of the slow component of the classical system with the local molecular environment replacing the viscosity. The environment of a set of phenyl groups involved in a particular motion is also composed of molecular librators, i.e., other phenyls, methyls, and components of the backbone. In most cases, a displaced oscillator will relax, reforming the initial local structure. However, occasionally, the simultaneous motions of several adjacent oscillators will block the return path and shift the local structure. This is like the sudden jumps that are seen in molecular dynamics simulations[51] and represents a single step in the evolution of the structure. The collection of these steps, which will have a broad distribution of step rates, is the α relaxation.

As the temperature is reduced, the β relaxation does not change its time dependence since it is relaxation on local potential surfaces that are fixed on the β relaxation time scale. However, the probability that a step in the α relaxation will occur is greatly reduced since a single step requires the simultaneous excitation of a number of oscillators with the proper correlation of motions to couple to a mode responsible for the structural change. At low enough temperature, the probability of a significant number of such steps occurring on any reasonable experimental time scale becomes vanishingly small, and α relaxation ceases to occur. The temperature at which this occurs is to some extent dependent on the time scale of the experimental observable. At sufficiently high temperature, the time scale for the loss of the local structure becomes comparable to the time for relaxation on the potential surface,[13,19,36] all dynamics are coupled. Even the fast relaxations becomes temperature dependent, and β relaxation ceases to exist.

IV. CONCLUDING REMARKS

Unlike many simple liquids, the PMPS phenyl group orientational relaxation does not follow the DSE equation and the dynamics are decoupled from the low-frequency hydrodynamic modes. On a time scale longer than that examined in these experiments, PMPS displays temperature-dependent dynamics, e.g., the temperature dependence of Brillouin linewidth and the observed Vogel–Fulcher–Tammann temperature dependence of the viscosity.

The temperature-independent nature of the dynamics and the local character of the dynamics are distinctive features of β relaxation in glass forming liquids.[3,4] In scattering experiments on glass forming liquids near the glass transition temperature, a Rayleigh peak is observed, a Boson peak is observed, and a broad spectral feature between the peaks is seen.[3,24] A narrow Rayleigh peak arises from the slow orientational motions of the liquid; the Boson peak comes from low-frequency phonon modes which include librations.[3,24,56,57] The spectrum of the broad feature is temperature independent, and is ascribed to β relaxation.[3,52] In transient grating experiments, the equivalent of the Rayleigh peak is slow temperature-dependent decays as observed in bipheny[16] and other simple liquids. The equivalent of the Boson peak is the ultrafast (< 1 ps) librational dynamics. Because of the large dynamic range and broad time scale examined in the TGOKE experiments, the ultrafast librational dynamics do not interfere with the observation of the fast time scale dynamics. It is

proposed that the temeprature-independent orientational dynamics of PMPS observed with the TGOKE experiments result from relaxation on local potential surfaces that are fixed on the time scale of the dynamics under observation. The observed dynamics contribute to the broad temperature-independent β relaxation feature seen in various scattering experiments.

ACKNOWLEDGMENT

This work was supported by the National Science Foundation, Division of Materials Research (No. DMR90-22675).

[1] D. Kivelson, in *Rotational Dynamics of Small and Macromolecules*, edited by T. Dorfmuller and R. Pecora (Springer, Berlin, 1987), p. 1.
[2] (a) E. Leutheusser, Phys. Rev. A **29**, 2765 (1984); (b) D. Bengtzelius, *ibid.* **34**, 5059 (1986); (c) W. Gotze and L. Sjogren, J. Phys. Condensed Matter **1**, 4183, 4203 (1989).
[3] M. Kruger, M. Soltwisch, I. Petscherizin, and D. Quitmann, J. Chem. Phys. **96**, 7352 (1992).
[4] (a) A. Sjolander, in *Static and Dynamic Properties of Liquids*, edited by M. Davidovic and A. K. Soper, Springer Proc. in Physics 40 (Springer, Berlin, 1989), p. 90. (b) M. Elmroth, L. Börjesson, and L. M. Torell, *ibid.* 118 (1989).
[5] C. A. Angell, in *Relaxations in Complex Systems*, edited by K. Nagai and G. B. Wright (National Technical Informaton Service, U.S. Department of Commerce, Springfield, VA, 1985), Vol. 1; J. Non-Cryst. Solids **73**, 1 (1985).
[6] D. Boese, B. Momper, G. Meier, F. Kremer, J. U. Hagenah, and E. W. Fischer, Macromolecules **22**, 4416 (1989).
[7] B. Frick, Progr. Colloid Polym. Sci. **80**, 164 (1989).
[8] G. Meier, F. Fujara, and W. Petry, Macromolecules **22**, 4421 (1989).
[9] J. P. Boon and S. Yip, *Molecular Hydrodynamics* (Dover, New York, 1991).
[10] S. Dattagupta, *Relaxation Phenomena in Condensed Matter Physics* (Academic, New York, 1987).
[11] D. Samios and T. Dorfmuller, Chem. Phys. Lett. **117**, 165 (1985).
[12] (a) Y. X. Yan and K. A. Nelson, J. Chem. Phys. **87**, 6240, 6257 (1987); (b) Y. X. Yan, L. F. Cheng, and K. A. Nelson, Adv. Infrared Raman Spectrosc. **16**, 299 (1987).
[13] J. J. Stankus, R. Torre, and M. D. Fayer, J. Phys. Chem. **97**, 9478 (1993).
[14] A. Sengupta, M. Terazima, and M. D. Fayer, J. Phys. Chem. **96**, 8619 (1992).
[15] V. J. Newell, F. W. Deeg, S. R. Greenfield, and M. D. Fayer, Opt. Soc. Am. B **6**, 257 (1989).
[16] F. W. Deeg, J. J. Stankus, S. R. Greenfield, V. J. Newell, and M .D. Fayer, J. Chem. Phys. **90**, 6893 (1989).
[17] J. Etchepare, G. Grillon, J. P. Chambaret, G. Hamoniaux, and A. Orszag, Opt. Commun. **63**, 329 (1987).
[18] F. W. Deeg and M. D. Fayer, J. Chem. Phys. **91**, 2269 (1989).
[19] S. R. Greenfield, A. Sengupta, J. J. Stankus, and M. D. Fayer, Chem. Phys. Lett. **193**, 49 (1992).
[20] S. Ruhman, L. R. Williams, A. G. Joly, B. Kohler, and K. A. Nelson, J. Phys. Chem. **91**, 2237 (1987).
[21] B. Kohler and K. A. Nelson, J. Phys. Condensed Matter **2**, SA109 (1990).
[22] M. Ito and T. Shigeoka, Spectrochim. Acta **22**, 1029 (1966).
[23] (a) B. C. Xu and R. M. Stratt, J. Chem. Phys. **92**, 1923 (1990); (b) G. Seeley and T. Keyes, *ibid.* **91**, 5581 (1989); (c) T. M. Wu and R. F. Loring, *ibid.* **97**, 8568 (1992).
[24] V. Z. Gochiyaev, V. K. Malinovsky, V. N. Novikov, and A. P. Sokolov, Philos. Mag. B **63**, 777 (1991).
[25] P. A. Madden, in *Molecular Liquids–Dynamics and Interactions*, edited by A. J. Barnes, W. J. Orville-Thomas, and J. Yarwood (Reidel, Dordrecht, 1984), p. 431.
[26] L. C. Geiger and B. M. Landanyi, Chem. Phys. Lett. **159**, 413 (1989).
[27] (a) L. D. Landau and E. M. Lifshitz, *Statistical Physics*, 3rd ed. (Pergamon, Oxford, 1980), Part 1, p. 377–389; (b) L. E. Reichl, *A Modern Course in Statistical Physics* (University of Texas, Austin, 1984), p. 545–556.
[28] B. J. Berne and R. Pecora, *Dynamic Light Scattering* (Wiley, New York, 1976).
[29] H. C. Anderson and R. Pecora, J. Chem. Phys. **54**, 2584 (1971); **55**, 1496 (1971).
[30] C. H. Wang, R. J. Ma, G. Fytas, and T. Dorfmuller, J. Chem. Phys. **78**, 5863 (1983).
[31] C. H. Wang and J. Zhang, J. Chem. Phys. **85**, 794 (1986).
[32] (a) H. Vogel, Phys. Z **22**, 645 (1921); (b) G. S. Fulcher, J. Am. Ceram. Soc. **8**, 339 (1925).
[33] E. Rossler, Phys. Rev. Lett. **65**, 1595 (1990).
[34] C. H. Wang, G. Fytas, and J. Zhang, J. Chem. Phys. **82**, 3405 (1985).
[35] C. H. Wang, R. J. Ma, and Q. L. Liu, J. Chem. Phys. **80**, 617 (1984).
[36] F. W. Deeg, S. R. Greenfield, J. J. Stankus, V. J. Newell, and M. D. Fayer, J. Chem. Phys. **93**, 3503 (1990).
[37] W. Steffen, A. Patkowski, G. Meier, and E. W. Fischer, J. Chem. Phys. **96**, 4171 (1992).
[38] F. Kremer, D. Boese, G. Meier, and E. W. Fischer, Progr. Colloid Polym. Sci. **80**, 129 (1989).
[39] The 0.7 ps decay is fast enough to have a contribution from interaction induced polarizability. The slowest component of the librational decay is ~70 fs. Therefore the 0.7 ps decay is distinct from the librational decay. The 1.95 ps melt decay, which runs out to 10 ps, is probably too slow to arise from interaction induced effects.
[40] L. A. Dissado, R. R. Nigamatullin, and R. M. Hill, Adv. Chem. Phys. **63**, 253 (1985).
[41] J. Frenkel, *Kinetic Theory of Liquids* (Dover, New York, 1955).
[42] R. C. Weast, *Handbook of Chemistry and Physics*, 67th ed. (Chemical Rubber, Boca Rotan, 1986-87), p. A-61.
[43] K. A. Littau, M. A. Dugan, S. Chen, and M. D. Fayer, J. Chem. Phys. **96**, 3484 (1992).
[44] K. A. Littau and M. D. Fayer, Chem. Phys. Lett. **176**, 551 (1991).
[45] R. G. Palmer, D. L. Stein, E. Abrahams, and P. W. Anderson, Phys. Rev. Lett. **53**, 958 (1984).
[46] Ajay and R. G. Palmer, J. Phys. A **23**, 2139 (1990).
[47] J. Klafter and M. F. Shlesinger, Proc. Natl. Acad. Sci. **83**, 848 (1986).
[48] B. A. Huberman and M. Kerszberg, J. Phys. A **18**, L331 (1985).
[49] D. Kumar and S. R. Shenoy, Solid State Commun. **57**, 927 (1986).
[50] S. Teitel and E. Domany, Phys. Rev. Lett. **55**, 2176 (1985).
[51] G. Fytas, Y. H. Lin, and B. Chu, J. Chem. Phys. **74**, 3131 (1981).
[52] D. Richter, B. Frick, and B. Farago, Phys. Rev. Lett. **61**, 2465 (1988).
[53] G. Floudas, J .S. Higgins, and G. Fytas, J. Chem. Phys. **96**, 7672 (1992).
[54] J. L. Barrat and M. L. Klein, Annu. Rev. Phys. Chem. **42**, 23 (1991).
[55] L. D. Landau and E. M. Lifshitz, *Mechanics*, 3rd ed. (Pergamon, Oxford, 1988), p. 76.
[56] R. Shuker and R. W. Gammon, Phys. Rev. Lett. **25**, 222 (1970).
[57] A. J. Martin and W. Brenig, Phys. Status Solidi B **64**, 163 (1974).